NOTES

Poliovirus Induces Apoptosis in the Mouse Central Nervous System

SOPHIE GIRARD,[1] THÉRÈSE COUDERC,[1]* JOSETTE DESTOMBES,[2] DANIÈLE THIESSON,[2] FRANCIS DELPEYROUX,[3] AND BRUNO BLONDEL[1]*

Unité de Neurovirologie et Régénération du Système Nerveux[1] and Laboratoire d'Epidémiologie Moléculaire des Entérovirus,[3] Institut Pasteur, 75724 Paris cedex 15, and URA CNRS 2115, Laboratoire du Cytosquelette et Développement, Faculté de Médecine Pitié-Salpétrière, 75634 Paris cedex 13,[2] France

Poliovirus (PV) is the etiological agent of human paralytic poliomyelitis. Paralysis results from the destruction of motoneurons, a consequence of PV replication. However, the PV-induced process leading to the death of motoneurons is not well known. We investigated whether PV-induced central nervous system (CNS) injury is associated with apoptosis by using mice as animal models. Transgenic mice expressing the human PV receptor were infected intracerebrally with either the neurovirulent PV-1 Mahoney strain or a paralytogenic dose of the attenuated PV-1 Sabin strain. Nontransgenic mice were infected with a mouse-adapted PV-1 Mahoney mutant. DNA fragmentation was demonstrated in CNS tissue from paralyzed mice by visualization of DNA oligonucleosomal laddering and by enzyme-linked immunosorbent assay. Viral antigens and DNA fragmentation detected by the in situ terminal deoxynucleotidyltransferase-mediated dUTP-biotin nick end-labeling technique were colocalized in neurons of spinal cords from paralyzed mice. In addition, morphological changes characteristic of cells undergoing apoptosis were observed in motoneurons by electron microscopy. Thus, we show that PV multiplication and CNS injury during paralytic poliomyelitis are associated with apoptosis.

Poliovirus (PV), an enterovirus belonging to the family *Picornaviridae*, is the etiological agent of paralytic poliomyelitis in humans. It is classified into three serotypes (PV-1, PV-2, and PV-3). The viral particle has a capsid composed of four proteins, VP1 to VP4, enclosing a single-stranded RNA of positive polarity.

PV first infects the oropharynx and the gut, is then released into the blood, and finally reaches the central nervous system (CNS). PV has a predilection for the motoneurons of the anterior horn of the cervical and lumbar regions of the spinal cord. In the brain, PV infection mostly involves the brain stem, notably the motor nuclei. Neuronal lesions in the forebrain are usually mild (4). The destruction of motoneurons, a consequence of PV replication, results in paralysis. However, the process by which PV causes CNS injury and the death of motoneurons is not well characterized. Experimentally, poliomyelitis can be transmitted to monkeys and, in some cases, to mice by inoculation of PV directly into the CNS. Monkeys and transgenic mice expressing the human PV receptor (TgPVR) are susceptible to wild strains of all three PV serotypes and, with a lower sensitivity, to attenuated strains (15, 26). In TgPVR mice, infection of the CNS is usually extensive and most often results in fatal poliomyelitis. In non-TgPVR mice, only a small number of PV strains induce poliomyelitis.

Cell damage in the CNS that is caused by its response to a virus infection can involve apoptosis (29). This has been illustrated in vivo with human and murine RNA neurotropic viruses, including human immunodeficiency virus (25), human T-cell leukemia virus type 1 (33), reovirus (22), La Crosse virus (24), rabies virus (13), mouse hepatitis virus (19), dengue virus (9), Sindbis virus (16), Venezuelan equine encephalitis virus (14), and Theiler's murine encephalomyelitis virus (32), a member of the *Picornaviridae* family. Among the other picornaviruses, coxsackievirus B3 (6) and hepatitis A virus (5) have been shown to induce apoptosis in cell cultures. PV can also induce or inhibit apoptosis in vitro according to the conditions of the viral infection (30, 31).

Apoptosis is essential for tissue homeostasis and embryonic development (23). It is an active process of cell death characterized by particular morphological and biochemical features, including chromatin condensation, nuclear and cell shrinkage, membrane blebbing, and oligonucleosomal DNA fragmentation. Apoptosis usually involves the rapid phagocytosis of affected cells without the release of proinflammatory cytokines (28). The dysregulation of apoptosis in humans results in a wide variety of diseases, notably cancers, autoimmune diseases, and neurodegenerative and neurodevelopmental disorders (2, 27). However, apoptosis may be an important host defense mechanism for eliminating infected cells during viral infection. Nevertheless, virus-induced activation of apoptosis in nonrenewable cells, like neurons, may result in an irreversible pathology. Therefore, it would be interesting to know whether the death of motoneurons leading to paralytic poliomyelitis involves an apoptotic process.

To determine whether the cytopathic effect of PV in the CNS was associated with apoptosis during paralytic poliomyelitis, we analyzed DNA fragmentation in the CNS of TgPVR mice in-

---

* Corresponding author. Mailing address: Unité de Neurovirologie et Régénération du Système Nerveux, Institut Pasteur, 28 rue du Docteur Roux, 75724 Paris cedex 15, France. Phone: (33) 1.45.68.87.62. Fax: (33) 1.40.61.34.21. E-mail: bblondel@pasteur.fr and tcouderc@pasteur.fr.
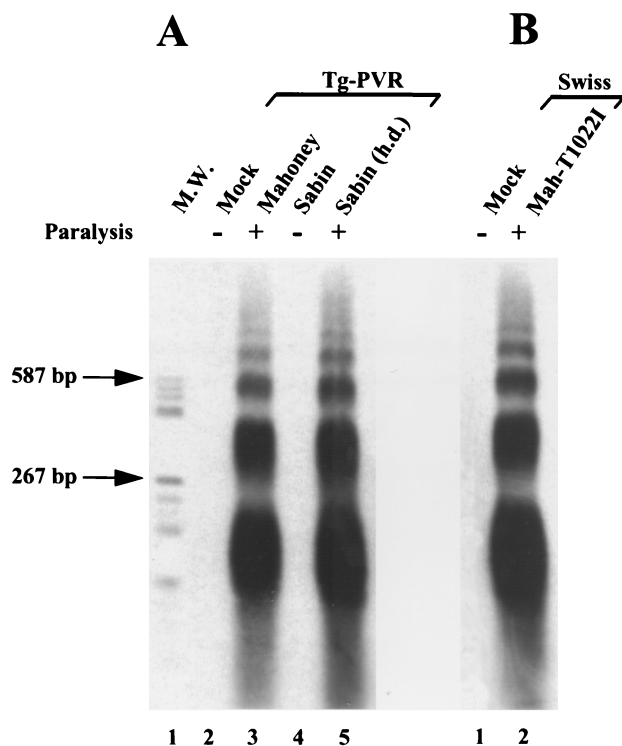
A   B

FIG. 1. Detection of DNA ladders in spinal cords from PV-infected TgPVR (A) and nontransgenic Swiss (B) mice. (A) Lane 1, DNA molecular weight (M.W.) markers; lanes 2 and 3, TgPVR mice 3 days after mock inoculation and inoculation of 2.5×10^4 PFU of PV-1 Mahoney, respectively; lanes 4 and 5, TgPVR mice 4 days after injection of 2.5×10^4 PFU of attenuated PV-1 Sabin and of a higher dose (h.d.) corresponding to 1.5×10^8 PFU, respectively. (B) Lane 1, Swiss mice 4 days after mock inoculation; lane 2, Swiss mice 4 days after inoculation of 6×10^7 PFU of mouse-adapted PV-1 Mah-T1022I.

fected with PV-1 Mahoney. In particular, we tested for oligonucleosomal laddering, an indicator of apoptosis. Five- to seven-week-old TgPVR mice were inoculated intracerebrally with either 2.5×10^4 PFU (100 50% paralytic doses) of the PV-1 Mahoney strain in 0.03 ml of phosphate-buffered saline (PBS) or with PBS alone as a negative control. Mouse spinal cords were removed on day 3, the time at which paralysis starts. Spinal cord homogenates (10% [wt/vol]) were prepared in isotonic buffer (200 mM KCl, 50 mM HEPES, 1 mM EGTA, and 1 mM $MgCl_2$) at 4°C with micropilons. The homogenates were centrifuged at $13,000 \times g$ for 20 min at 4°C, and then supernatants, which contained low-molecular-weight DNA, were collected and stored at -80°C. For each sample, 0.3 ml of supernatant (corresponding to 30 mg of tissue) was deproteinized by treatment with proteinase K (2 μg) for 30 min at 37°C and was extracted twice with phenol-chloroform. The supernatants were then treated with RNase A (2.5 μg) for 15 min at 37°C. After phenol-chloroform extraction, DNA was precipitated and end labeled with terminal transferase (25 U) and digoxigenin-11-ddUTP (50 μM final concentration) (Boehringer Mannheim) in a volume of 16 μl, according to the manufacturer's instructions. The samples were electrophoresed on a 1.8% agarose gel, transferred to a Hybond-N nylon membrane (Amersham Life Science), and visualized by the digoxigenin luminescent detection kit (Boehringer Mannheim) with alkaline phosphatase-conjugated antibody and Lumi-phos Plus as the chemiluminescent substrate for alkaline phosphatase. A distinct DNA laddering pattern, consisting mainly of mono- (180- to 200-bp), di-, and trinucleosome fragments, was observed in the spinal cords of paralyzed TgPVR mice (Fig. 1A, lane 3). No such lad-

dering was observed in the spinal cords of control TgPVR mice inoculated with PBS alone (Fig. 1A, lane 2). Thus, PV infection caused cleavage of DNA into nucleosomes in the mouse CNS.

To analyze the time course of apoptosis in the mouse CNS, DNA fragmentation was evaluated daily with a quantitative enzyme-linked immunosorbent assay (ELISA). The CNS was removed from at least three TgPVR mice inoculated with PV-1 Mahoney as described above immediately and 1, 2, 3, 4, and 5 days after infection. The CNS was dissected into three parts: forebrain (cerebral hemispheres and diencephalon), brain stem (midbrain, pons, cerebellum, and medulla), and spinal cord. All tissues were stored at -80°C. Tissue homogenates, 10% (wt/vol) for the spinal cord and brain stem and 20% (wt/vol) for the forebrain, were prepared in isotonic buffer and centrifuged as described above. Aliquots of 20 μl of supernatants were used for ELISA according to the manufacturer's instructions (Cell Death Detection ELISA[plus]; Boehringer Mannheim). Briefly, this technique utilizes a histone-specific monoclonal antibody to capture oligonucleosomal DNA fragments present in the samples. The captured DNA fragments are detected with a peroxidase-conjugated anti-DNA monoclonal antibody and quantitated at 410 nm in a spectrophotometer (Dynatech MR5000). Substantial DNA fragmentation was detected in the spinal cords and brain stems of infected TgPVR mice on and after day 3 postinfection, by which time paralysis had started (Fig. 2A). Although the values were variable, the concentration of oligonucleosomes was generally higher in the spinal cords than in the brain stems. Only minor oligonucleosomal DNA fragmentation was detected in the forebrains of infected mice, and it was detected only on day 3. Because the spinal cord is the region of the CNS most severely affected by PV infection and because forebrain centers are generally spared during poliomyelitis (4, 15, 26), it seems that apoptosis occurred specifically in the CNS area where viral replication is most efficient.

To investigate whether the time course of apoptosis correlates with that of viral growth, the viral load was determined in homogenate supernatants of the forebrain, brain stem, and spinal cord by measuring 50% tissue culture infectious doses ($TCID_{50}$) on HEp-2c cell cultures (21). The maximum virus titer in the brain stem and in the spinal cord was reached on day 3 (Fig. 2B). Maximal virus growth was higher in the spinal cord and brain stem than in the forebrain. The low concentration of oligonucleosomes in the forebrain thus correlated with a lower viral replication in this CNS area. These experiments demonstrate that apoptosis as detected by ELISA coincided with maximal virus growth in the spinal cord and brain stem and with the onset of paralysis.

To determine whether the attenuated strain of PV-1 could trigger apoptosis in the CNS, TgPVR mice were injected with a paralytogenic dose of PV-1 Sabin (1.5×10^8 PFU) (15) and with the same dose as that inoculated for the neurovirulent PV-1 Mahoney strain (2.5×10^4 PFU). All mice inoculated with the highest dose of PV-1 Sabin were paralyzed 3 or 4 days after infection. No mice injected with the lowest dose developed clinical disease. A DNA ladder was detected only in the spinal cords of paralyzed mice (Fig. 1A, lanes 4 and 5), and as expected, viral growth could be detected only in the spinal cords of these mice (about 10^7 $TCID_{50}$/g). These findings show that the attenuated PV-1 Sabin strain, when replicating at a sufficient level, can kill cells of the CNS by an apoptotic process as does the neurovirulent strain of PV-1. Thus, as previously shown for Theiler's murine encephalomyelitis virus and Sindbis virus, the detection of apoptosis correlated with a level of PV multiplication generating paralysis (17, 32) for both a neurovirulent and an attenuated PV strain. However, we cannot exclude the possibility that high doses of the PV-1 Sabin strain
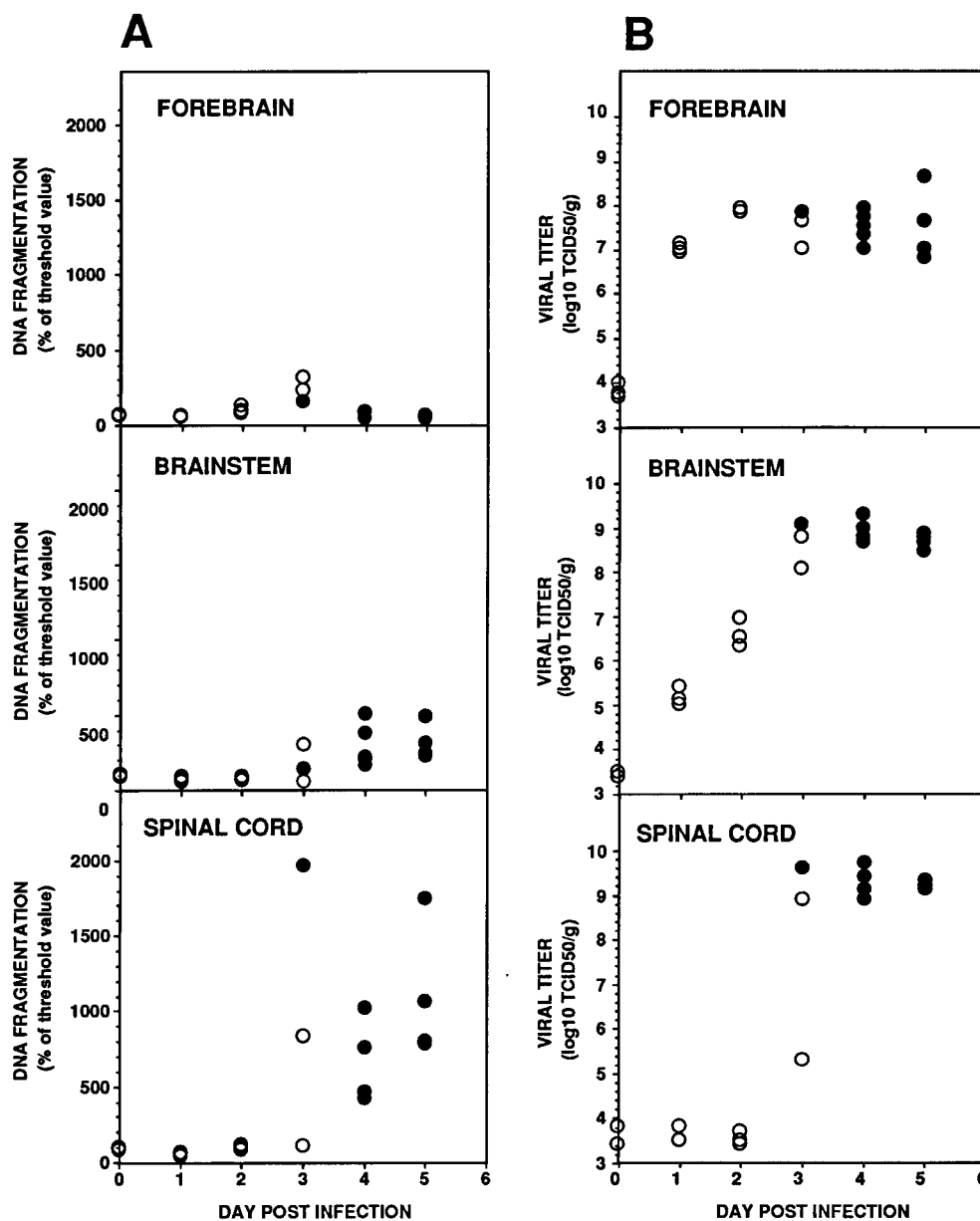
FIG. 2. DNA fragmentation analysis by ELISA (A) and PV production (B) in homogenate supernatants of the forebrains, brain stems, and spinal cords of PV-1 Mahoney-infected TgPVR mice. Nonparalyzed mice (open circles) and paralyzed infected mice (solid circles) are indicated. The threshold value for the ELISA was set as the mean value for two negative controls plus twice the standard error of the mean. The viral titer of each homogenate supernatant was determined by $TCID_{50}$ measurements on HEp-2c cell cultures (21).

induced apoptosis due to the presence of a few mutants in the viral stock that were able to replicate in the CNS.

To determine if cells dying by apoptosis were infected with PV, frozen longitudinal tissue sections (10 μm thick) fixed in periodate-lysine-paraformaldehyde solution (20) were prepared from the spinal cords of paralyzed TgPVR mice following injection of PV-1 Mahoney. The samples were subjected to both terminal deoxynucleotidyltransferase-mediated dUTP nick end labeling (TUNEL) and immunostaining for viral antigens. TUNEL reactions were performed on tissue sections with biotin-16-dUTP (Boehringer Mannheim) and streptavidin-CY3 conjugate (Jackson Immunoresearch) to end label the DNA at strand breaks. PV antigens were detected with a mouse monoclonal

antibody (C3) directed against the PV capsid (3) and with fluorescein isothiocyanate-conjugated rabbit anti-mouse immunoglobulin G (Sanofi Diagnostic Pasteur). Immunostaining for viral antigens and TUNEL assays on sections of spinal cords from mice inoculated with PBS alone were uniformly negative (Fig. 3D). In sections from paralyzed TgPVR mice, antigen-positive cells were scattered throughout the spinal cord gray matter, as previously reported (15, 26), and their location, size, and morphology were consistent with those of neuronal cells. In the anterior horn, some of the infected cells could be identified as large motoneurons (Fig. 3A and B). The antigen staining was specifically located in the cell cytoplasm, the site of PV replication. The TUNEL assay indicated that 76% (706 of 928) of the infected neurons had nuclei
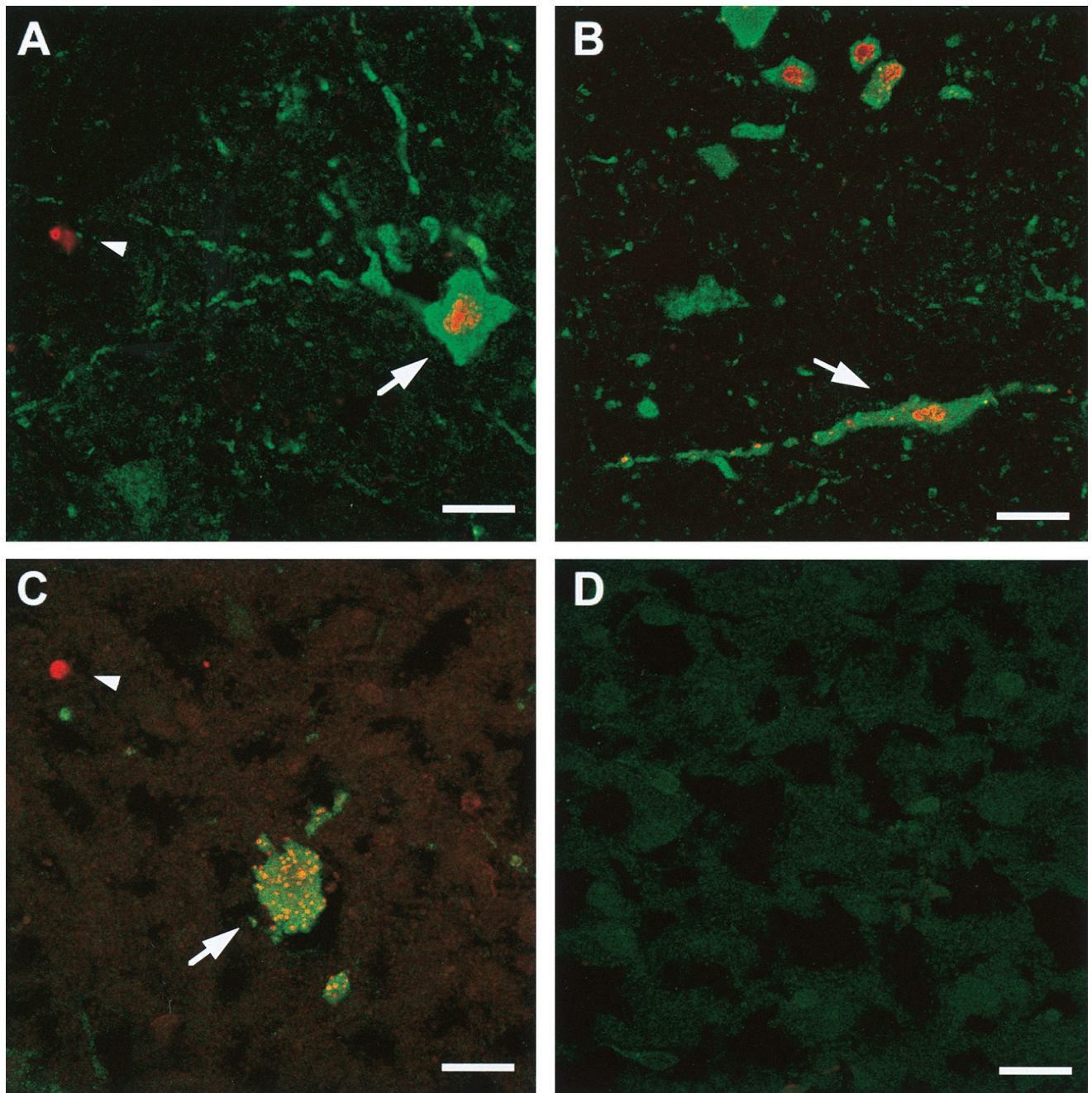
FIG. 3. Immunofluorescent codetection of apoptosis and viral antigens in spinal cords from PV-1-infected TgPVR and nontransgenic Swiss mice. Immunostaining for viral antigen (green) and TUNEL labeling for DNA fragmentation (red) were performed on longitudinal sections through the ventral horn of spinal cords taken from paralyzed mice. (A and B) TgPVR mice 4 days after infection with PV-1 Mahoney; (C) Swiss mouse 2 days after infection with PV-1 Mah-T1022I; (D) TgPVR mouse 3 days after mock infection. Large infected motoneurons exhibiting nuclear condensation (arrow) and apoptotic nuclei from noninfected bystander cells (arrowheads) are indicated. Bars, 20 μm.

exhibiting a morphology unique to apoptosis, including nuclear fragmentation (Fig. 3A and B). We also observed TUNEL-positive nuclear fragments surrounded by a rim of PV antigen-positive cytoplasm (not shown). This image was consistent with apoptotic bodies resulting from disintegration of infected neurons. Surprisingly, the gray matter, as well as the white matter of the spinal cord near the area of infected neurons, contained cells that were positive for chromatin condensation but negative for viral immunostaining (Fig. 3A). Although these cells remain to be

identified, their location and the size of their nuclei suggested that they were glial or inflammatory cells rather than neurons. Furthermore, inflammatory cell infiltration could be observed after cresyl violet staining of similar sections (Fig. 4) embedded in paraffin as previously described (10). Classical chromatolysis of most neurons was also revealed by dark staining of Nissl bodies in the affected areas.

The morphological changes of neurons in the spinal cords of paralyzed TgPVR mice infected with PV-1 Mahoney were
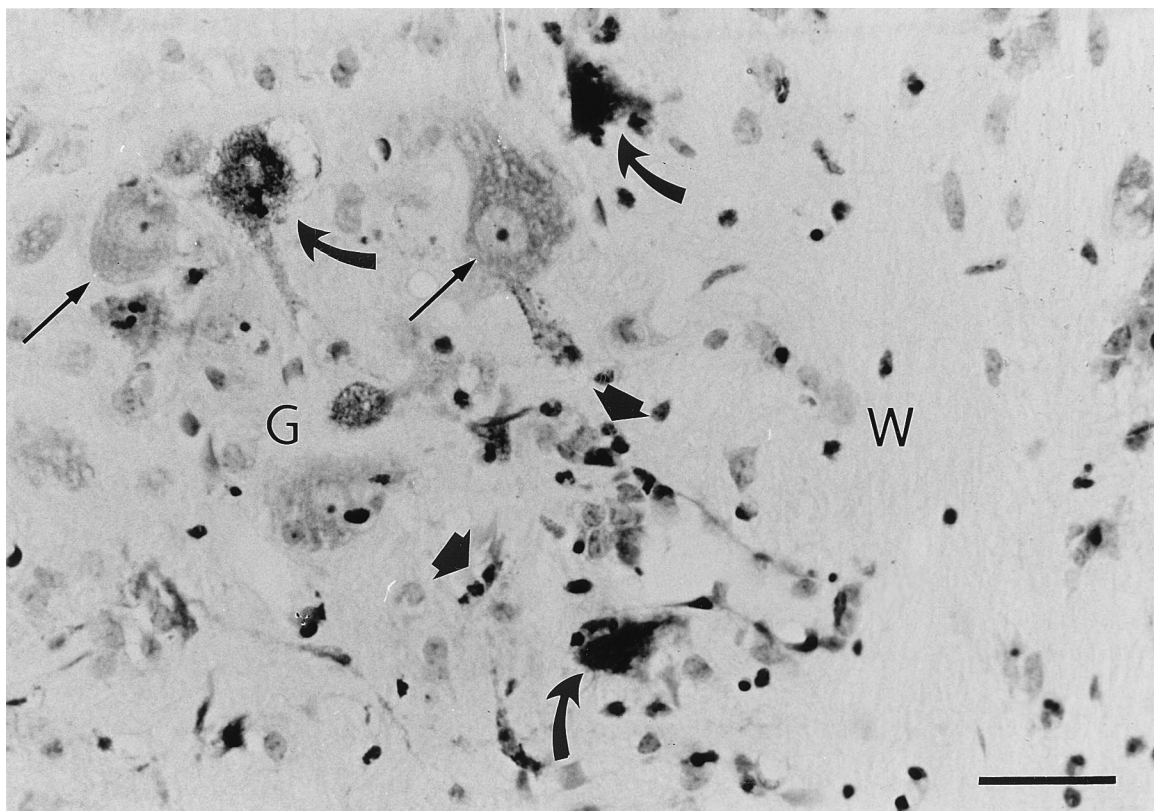
FIG. 4. Cresyl violet staining of longitudinal section through the ventral horn of the spinal cord from a TgPVR mouse 4 days after infection with PV-1 Mahoney. Chromatolyzed (curved arrows) and nonchromatolyzed (thin arrows) neurons are indicated, as well as inflammatory cells (large arrows). Gray (G) and white (W) matter are labelled. Bar, 20 μm.

assessed by electron microscopy. Sections of the spinal cord were treated as previously described (10). Various specific morphological ultrastructural alterations that occur during apoptosis were observed specifically in the CNS of infected mice but not in those of mock-infected mice (Fig. 5). Neurons showed shrinkage, membrane blebbing, and abnormally convoluted nuclear outlines. The chromatin was condensed and collapsed into crescents at the periphery of the nucleus (Fig. 5B). At later stages, there was vacuolation and disorganization of the cytoplasm. The nucleus appeared more indented, and discrete nuclear fragments were sometimes present (Fig. 5C). Moreover, the nucleolus was enlarged, and its granules were coarse and abnormally scattered (not shown). Finally, the nucleus was fragmented, although the cell membrane was still present with a marked blebbing (Fig. 5D).

Altogether, the data obtained with TgPVR mice as the animal model showed that PV multiplication and CNS injury during paralytic poliomyelitis were associated with apoptosis. To investigate whether PV triggers apoptosis in nerve cells that do not express the human PV receptor, we tested for apoptosis in the CNS of nontransgenic Swiss mice (OF1; Iffa-Credo) infected with a mouse-adapted PV strain. We had previously isolated and characterized a mouse-adapted PV mutant, PV-1 Mah-T1022I (formerly named Mah-KK/NK-VP1 [8] or KKVP1I22 [7]), derived from PV-1 Mahoney. This mutant is paralytogenic in non-TgPVR mice. Furthermore, most nontransgenic mice inoculated with PV-1 Mah-T1022I survive after the onset of paralysis (10), while TgPVR mice developing paralysis following PV inoculation die. Five-week-old Swiss mice were inoculated intracerebrally with 6×10^7 PFU of PV-1 Mah-T1022I, and spinal cords were re-

moved on the day of onset of paralysis (day 3 or 4 postinfection). As shown in Fig. 1B (lane 2), a DNA ladder was detected in spinal cord samples from the paralyzed nontransgenic Swiss mice, indicating that the mouse-adapted strain of PV-1 induced oligonucleosomal fragmentation in the CNS of Swiss mice independently of human PV receptor expression. The intensity of the DNA ladder visualized in Swiss mice was equivalent to that in the ladders detected in TgPVR mice. However, this assay is not quantitative to a degree which would enable addressing the question of whether there is a correlation between apoptosis and the severity of the disease. Lumbar spinal cord sections from Swiss mice with a paralyzed hind limb were immunostained for viral antigen and analyzed by TUNEL assay. In contrast to TgPVR mice, antigen-positive cells were found only in the anterior horn of the lumbar spinal cord corresponding to the paralyzed muscle. The location, morphology, and size of most of these cells identified them as large motoneurons. Most of the antigen-positive neurons displayed severe cellular damage and gave a positive TUNEL signal (Fig. 3C). As was observed in infected TgPVR mice, some neurons with normal morphology and negative TUNEL scoring were antigen positive (data not shown). Moreover, some TUNEL-positive nonneuronal cells near the infected neurons were negative for viral immunostaining (Fig. 3C).

Our results in both TgPVR and Swiss mice indicate that virus-induced apoptosis is an important component of PV-induced cell death and tissue injury in the CNS of infected mice leading to paralysis. In the CNS of paralyzed mice, most infected neurons died by apoptosis. However, some infected neurons presented a normal morphology and did not exhibit apoptotic nuclei. These may have been neurons which were infected but had not yet
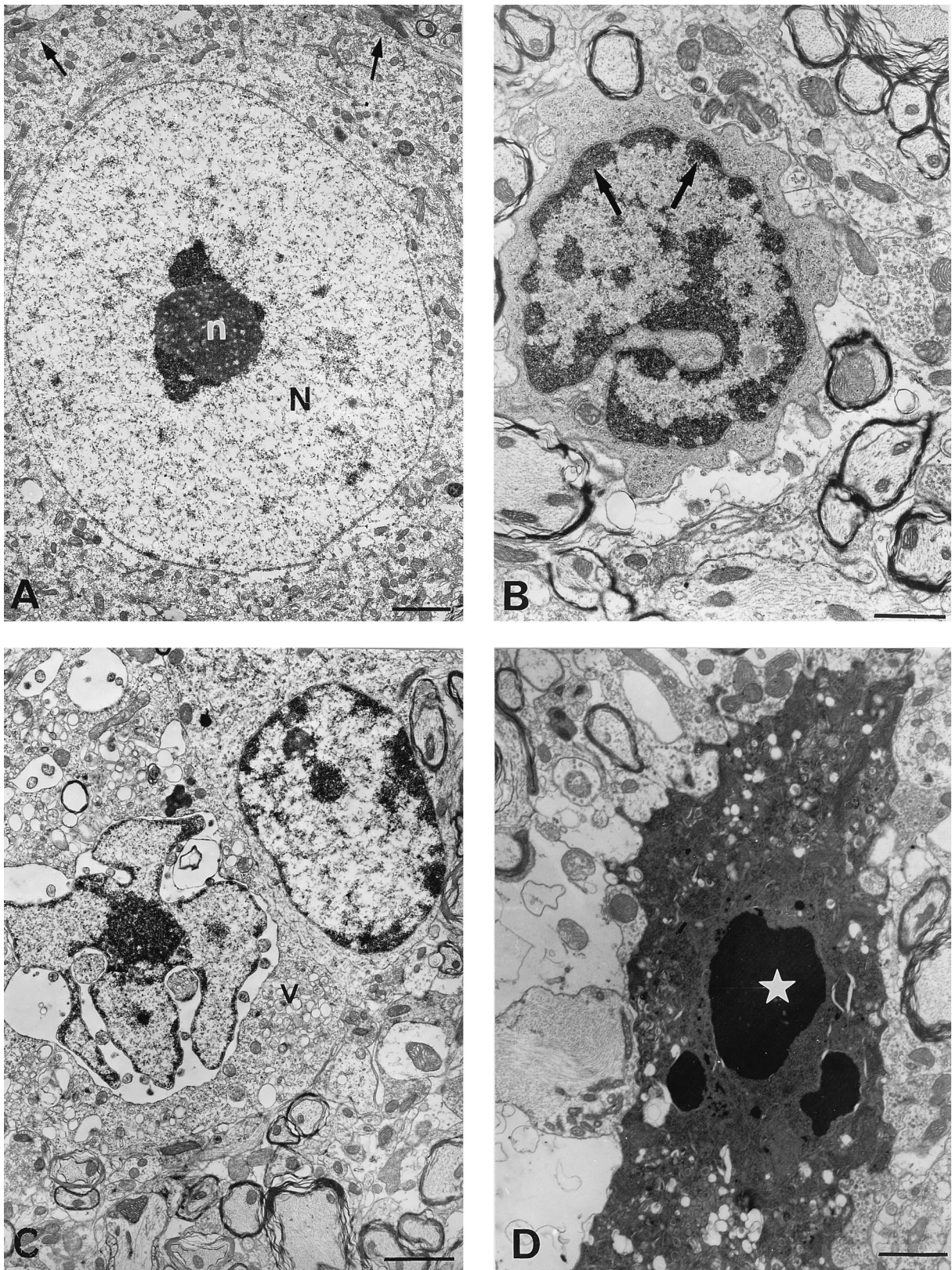
FIG. 5. Electron micrographs of motoneurons in the spinal cords of PV-1 Mahoney-infected TgPVR mice. (A) Mouse 5 days after mock infection; (B through D) paralyzed mice 5 days after infection with PV-1 Mahoney. In the spinal cord from a mock-infected mouse, motoneurons display a round nucleus (N) with a single electron-dense nucleolus (n) (A). In PV-1 Mahoney-infected mice, the following specific morphological alterations consistent with apoptosis were observed in motoneurons: aggregates of chromatin (arrows) around the nuclear membrane, cytoplasmic condensation with severely distorted organelles, the cellular surface showing protusions (B), breaking up of the nucleus and overall compaction of the cytoplasm associated with the development of translucent cytoplasmic vacuoles (v) (C), and the cell finally breaking apart into a number of apoptotic bodies (star) (D). Bars, 5 μm (A) and 10 μm (B through D).

become apoptotic or reached the stage of DNA fragmentation. Alternatively, some neurons may be less sensitive to apoptosis. It would be interesting to know if these infected neurons recover from PV infection. This would be in agreement with Bodian's observations describing complete morphological recovery of some affected motor nerve cells in the monkey CNS following PV infection (4). Apoptosis was also observed in uninfected nonneuronal cells contiguous to the PV-infected neurons. Although these cells remain to be identified with certainty, they are probably glial or inflammatory cells. CNS injury may thus be enhanced by apoptosis in uninfected cells. These observations suggest that tissue damage associated with PV infection may result from the induction of apoptosis by a combination of direct and indirect mechanisms, as reported to be the case with other viral infections (12, 22). Indeed, it seems that PV-triggered apoptosis in neurons involved a direct mechanism, whereas apoptosis in uninfected nonneuronal bystander cells may involve an indirect mechanism. Unidentified factors from PV-infected neurons and/or inflammatory cells may play a role in the induction of apoptosis in these nonneuronal bystander cells. These factors could be secreted toxic viral gene products (18, 34) or proinflammatory cytokines and effector molecules resulting from immune activation (1, 35). Recent studies on experimental autoimmune encephalomyelitis suggest that the CNS can eliminate T-cell-dependent inflammation by apoptosis (11). It would therefore be interesting to determine whether the apoptotic nonneuronal bystander cells are T cells.

As previously shown, the mouse-adapted PV mutant, PV-1 Mah-T1022I, persists in the CNS of Swiss mice after the onset of paralysis (10). Furthermore, PV can induce or, in contrast, inhibit apoptosis in vitro according to the conditions of viral infections (31). Possibly, inhibition of apoptosis promotes persistence of PV. To address this issue, we are currently investigating whether apoptosis occurs during persistent infection.

REFERENCES

1. **Badley, A. D., J. A. McElhinny, P. J. Leibson, D. H. Lynch, M. R. Alderson, and C. V. Paya.** 1996. Upregulation of Fas ligand expression by human immunodeficiency virus in human macrophages mediates apoptosis of uninfected T lymphocytes. J. Virol. **70:**199–206.
2. **Bellamy, C. O. C., R. G. D. Malcomson, D. J. Harrison, and A. J. Wyllie.** 1995. Cell death in health and disease: the biology and regulation of apoptosis. Semin. Cancer Biol. **6:**3–16.
3. **Blondel, B., O. Akacem, R. Crainic, P. Couillin, and F. Horodniceanu.** 1983. Detection by monoclonal antibodies of an antigenic determinant critical for poliovirus neutralization present on VP1 and on heat inactivated virions. Virology **126:**707–710.
4. **Bodian, D.** 1949. Histopathologic basis of clinical findings in poliomyelitis. Am. J. Med. **6:**563–578.
5. **Brack, K., W. Frings, A. Dotzauer, and A. Vallbracht.** 1998. A cytopathogenic, apoptosis-inducing variant of hepatitis A virus. J. Virol. **72:**3370–3376.
6. **Carthy, C. M., D. J. Granville, K. A. Watson, D. R. Anderson, J. E. Wilson, D. Yang, D. W. C. Hunt, and B. M. McManus.** 1998. Caspase activation and specific cleavage of substrates after coxsackievirus B3-induced cytopathic effect in HeLa cells. J. Virol. **72:**7669–7675.
7. **Couderc, T., F. Delpeyroux, H. Le Blay, and B. Blondel.** 1996. Mouse adaptation determinants of poliovirus type 1 enhance viral uncoating. J. Virol. **70:**305–312.
8. **Couderc, T., J. Hogle, H. Le Blay, F. Horaud, and B. Blondel.** 1993. Molecular characterization of mouse-virulent poliovirus type 1 Mahoney mutants: involvement of residues of polypeptides VP1 and VP2 located on the inner surface of the capsid protein shell. J. Virol. **67:**3808–3817.
9. **Desprès, P., M.-P. Frenkiel, P.-E. Ceccaldi, C. Duarte dos Santos, and V. Deubel.** 1998. Apoptosis in the mouse central nervous system in response to infection with mouse-neurovirulent dengue viruses. J. Virol. **72:**823–829.
10. **Destombes, J., T. Couderc, D. Thiesson, S. Girard, S. G. Wilt, and B. Blondel.** 1997. Persistent poliovirus infection in mouse motoneurons. J. Virol. **71:**1621–1628.
11. **Gold, R., H. P. Hartung, and H. Lassmann.** 1997. T-cell apoptosis in autoimmune diseases: termination of inflammation in the nervous system and other sites with specialized immune-defense mechanisms. Trends Neurosci. **20:**399–404.
12. **Herbein, G., C. Van Lint, J. L. Lovett, and E. Verdin.** 1998. Distinct mechanisms trigger apoptosis in human immunodeficiency virus type 1-infected and in uninfected bystander T lymphocytes. J. Virol. **72:**660–670.
13. **Jackson, A. C., and J. P. Rossiter.** 1997. Apoptosis plays an important role in experimental rabies virus infection. J. Virol. **71:**5603–5607.
14. **Jackson, A. C., and J. P. Rossiter.** 1997. Apoptotic cell death is an important cause of neuronal injury in experimental Venezuelan equine encephalitis virus infection of mice. Acta Neuropathol. **93:**349–353.
15. **Koike, S., C. Taya, T. Kurata, S. Abe, I. Ise, H. Yonekawa, and A. Nomoto.** 1991. Transgenic mice susceptible to poliovirus. Proc. Natl. Acad. Sci. USA **88:**951–955.
16. **Levine, B., Q. Huang, J. T. Isaacs, J. C. Reed, D. E. Griffin, and J. M. Hardwick.** 1993. Conversion of lytic to persistent alphavirus infection by the bcl-2 cellular oncogene. Nature **361:**739–742.
17. **Lewis, J., S. L. Wesselingh, D. E. Griffin, and J. M. Hardwick.** 1996. Alphavirus-induced apoptosis in mouse brains correlates with neurovirulence. J. Virol. **70:**1828–1835.
18. **Li, C. J., D. J. Friedman, C. Wang, V. Metelev, and A. B. Pardee.** 1995. Induction of apoptosis in uninfected lymphocytes by HIV-1 Tat protein. Science **268:**429–431.
19. **Lin, M. T., S. A. Stohlman, and D. R. Hinton.** 1997. Mouse hepatitis virus is cleared from the central nervous system of mice lacking perforin-mediated cytolysis. J. Virol. **71:**383–391.
20. **McLean, I. W., and P. K. Nakane.** 1974. Periodate-lysine-paraformaldehyde fixative: a new fixative for immunoelectron microscopy. J. Histochem. Cytochem. **22:**1077–1083.
21. **Melnick, J. L., H. A. Wenner, and C. A. Philips.** 1979. Enteroviruses, p. 471–534. *In* E. H. Lennette and N. J. Schmidt (ed.), Diagnostic procedure for viral, rickettsial and chlamydial infections. American Public Health Association, Washington, D.C.
22. **Oberhaus, S. M., R. L. Smith, G. H. Clayton, T. S. Dermody, and K. L. Tyler.** 1997. Reovirus infection and tissue injury in the mouse central nervous system are associated with apoptosis. J. Virol. **71:**2100–2106.
23. **Oppenheim, R. W.** 1991. Cell death during development of the nervous system. Annu. Rev. Neurosci. **14:**453–501.
24. **Pekosz, A., J. Phillips, D. Pleasure, D. Merry, and F. Gonzalez-Scarano.** 1996. Induction of apoptosis by La Crosse virus infection and role of neuronal differentiation and human *bcl*-2 expression in its prevention. J. Virol. **70:**5329–5335.
25. **Petito, C. K., and B. Roberts.** 1995. Evidence of apoptotic cell death in HIV encephalitis. Am. J. Pathol. **146:**1121–1130.
26. **Ren, R. B., F. Costantini, E. J. Gorgacz, J. J. Lee, and V. R. Racaniello.** 1990. Transgenic mice expressing a human poliovirus receptor: a new model for poliomyelitis. Cell **63:**353–362.
27. **Rudin, C. M., and C. B. Thompson.** 1997. Apoptosis and disease: regulation and clinical relevance of programmed cell death. Annu. Rev. Med. **48:**267–281.
28. **Schwartzman, R. A., and J. A. Cidlowski.** 1993. Apoptosis: the biochemistry and molecular biology of programmed cell death. Endocr. Rev. **14:**133–151.
29. **Shen, Y., and T. E. Shenk.** 1995. Viruses and apoptosis. Curr. Opin. Genet. Dev. **5:**105–111.
30. **Tolskaya, E. A., T. A. Ivannikova, M. S. Kolesnikova, S. G. Drozdov, and V. I. Agol.** 1992. Postinfection treatment with antiviral serum results in survival of neural cells productively infected with virulent poliovirus. J. Virol. **66:**5152–5156.
31. **Tolskaya, E. A., L. I. Romanova, M. S. Kolesnikova, T. A. Ivannikova, E. A. Smirnova, N. T. Raikhlin, and V. I. Agol.** 1995. Apoptosis-inducing and apoptosis-preventing functions of poliovirus. J. Virol. **69:**1181–1189.
32. **Tsunoda, I., C. I. B. Kurtz, and R. S. Fujinami.** 1997. Apoptosis in acute and chronic central nervous system disease induced by Theiler's murine encephalomyelitis virus. Virology **228:**388–393.
33. **Umehara, F., A. Nakamura, S. Izumo, R. Kubota, N. Ijchi, N. Kashio, K.-I. Hashimoto, K. Usuku, E. Sato, and M. Osame.** 1994. Apoptosis of T lymphocytes in the spinal cord lesions in HTLV-I-associated myelopathy: a possible mechanism to control viral infection in the central nervous system. J. Neuropathol. Exp. Neurol. **53:**617–624.
34. **Westendorp, M. O., R. Frank, C. Ochsenbauer, K. Stricker, J. Dhein, H. Walczak, K. M. Debatin, and P. H. Krammer.** 1995. Sensitization of T cells to CD95-mediated apoptosis by HIV-1 Tat and gp120. Nature **375:**497–500.
35. **Zheng, L., G. Fisher, R. E. Miller, J. Peschon, D. H. Lynch, and M. J. Lenardo.** 1995. Induction of apoptosis in mature T cells by tumour necrosis factor. Nature **377:**348–351.